LASERS

PACS numbers: 42.55.Lt; 42.62.Cf
DOI: 10.1070/QE2002v032n03ABEH002175

Highly efficient repetitively pulsed electric-discharge industrial CO_2 laser

V.V.Osipov, M. G.Ivanov, V. V.Lisenkov, V.V.Platonov

Abstract. **The results of investigations aimed at the development of a repetitively pulsed CO_2 laser with an active medium volume of 1000 cm^3 pumped by a combined discharge are generalised. It is shown that, at pump pulse durations of 200 – 500 μs, the optimal characteristics are achieved at active-medium pressures of 60 – 100 Torr. In this case, the laser efficiency at the initial stage of its operation can reach 22 % and; if the energy dissipated in the region of the cathode potential drop is neglected, the efficiency is 28 %. After emission of 3×10^5 pulses, the laser efficiency falls to 12 %. It has been found that adding CO with a relative concentration $[CO]/[CO_2] \sim 0.75$ increases the input and output power by almost 50 %. The lasing efficiency is then 10 % – 12 %, and the service life of the laser is by more than 10^6 pulses with a power decrease of no more than 10 %. Adding hydrogen up to a concentration $[H_2]/[CO_2] \sim 10$ leads to an increase in the energy supplied to the gas due to a decrease in the rate of ionisation processes. However, the optimal ratio is $[H_2]/[CO_2] \sim 1$, at which the output power increases by 15 %. In a long-term operating mode, the laser power is 1 kW at a peak power of 10 kW and an efficiency of 12 %.**

Keywords: *CO_2 laser, repetitively pulsed oscillating mode, combined discharge.*

1. Introduction

At present, the problem of developing highly efficient scaled CO_2 lasers still remains important for solving technological problems and designing large-scale laser systems.

Such lasers, as a rule, continuously pumped, when the entire active medium circulated over the discharge volume is excited, which provides good energy parameters of the cw output. In a pulse regime, a larger part of the working gas is pumped through the discharge volume during the time interval between laser pulses and remains unexcited. Moreover, the problem of designing high-power repetitively pulse lasers is aggravated by the absence of high-power efficient and fast switches with a long service life.

However, repetitively pulsed radiation has a more significant effect on a target. For this reason, a search has been conducted for a long time for the methods of repetitively pulsed excitation of working media, which would provide high specific energy characteristics, scaling, and a high laser efficiency. The possibility of solving this problem was demonstrated by the development of CO_2 lasers pumped by a nonself-sustained discharge (NSSD), which is maintained by an electron beam [1]. These lasers have high specific energy characteristics and a high efficiency and are capable of operating in the cw and repetitively pulsed regimes, i.e., they satisfy completely the requirements of various technological processes. However, the use of such lasers in industry is hindered by the use of electron accelerators in them, which complicates the laser and leads to a radiation hazard and a short service life, because a metal foil separating the vacuum and gas-filled volumes is destroyed under the action of an electron beam.

The most promising way for solving this problem is to use a short-duration self-sustained discharge (SSD) for producing a plasma in the working volume instead of an electron beam. Such discharges, which were called combined [2], can be obtained by several methods that differ in the isolation of the feed circuits for the SSD and NSSD [3 – 8].

A disadvantage of these methods is the presence of elements in the feed circuits, which appreciably limit the current and specific energy characteristics of the combined discharge, or unequal conditions for the current flow in different interelectrode gaps [3].

This work presents the results of investigations of a repetitively pulsed CO_2 laser pumped by a combined discharge, whose excitation circuits have no elements that basically limit the SSD and NSSD currents.

2. Experimental complex

The electric-discharge industrial laser complex consists of the following basic components: a laser unit, a system for gas evacuation and admission, power supplies for the self-sustained and nonself-sustained discharges, and detecting electronics.

The dimensions of the laser unit are $100 \times 102 \times 120$ cm. A copper heat exchanger capable of utilising a heat power of 8 kW, an electrode system, and a diametric fan with a working wheel 40 cm in diameter driven by a 2PN-112 motor (3000 rpm) through a samarium – cobalt magnetic

V.V.Osipov, M.G.Ivanov, V.V.Lisenkov, V.V.Platonov Institute of Electrophysics, Ural Branch, Russian Academy of Sciences, ul. Amundsena 106, 620016, Ekaterinburg, Russia;
e-mail: max@iep.uran.ru

Received 14 May 2001; revision received 26 September 2001
Kvantovaya Elektronika **32** (3) 253 – 259 (2002)
Translated by A.S.Seferov

clutch, which ensures a gas flow velocity of up to 50 $m^{-1}s$ through the discharge zone, are enclosed in a stainless steel housing. A stable single-pass cavity consisting of a concave copper mirror (with a reflectivity of 98 % and a radius of curvature of 20 m) and a plane–parallel ZnSe plate (one of its faces had an antireflection coating, and the other had a reflectivity of 74 %) were mounted on the laser-unit housing.

A modified UZGB-04 (1.5–3 kV, $\sim$ 15 kW) and an IGLA-6 (4–10 kV, $\sim$ 500 W) power sources supplied the energy to the gas at the NSSD and SSD stages, respectively.

The radiation power was measured with a TPI-2M calorimeter and, through KCl beamsplitters with an IMO-2N calorimeter. The maximum radiation power was additionally monitored by measuring the water evaporation rate.

The discharge current and voltage were recorded with a Tektronix DS520A oscilloscope. The pressure in the gas mixture was measured with a 1227-type vacuum gauge. The gas circulation velocity was determined from the rotation velocity of the electric-motor rotor and calibrated with Pitot tubes.

The excitation circuits [9, 10] shown in Fig. 1 were used to initiate and maintain a combined discharge.

The laser working zone was preionised by a multichannel diffusive discharge [11] excited in the gap between one of the main electrodes and a sectioned ignitor electrode, which was placed at a distance of 0.5 cm upstream the gas flow. In both circuit versions, a short-duration (10^{-7} s) SSD was initiated in the interelectrode gap. After this discharge terminated, a longer (2×10^{-4} s) NSSD was initiated at the plasma decay stage. The duration of the latter discharge could be increased by applying additional SSD pulses maintaining the plasma in the discharge gap in a time shorter than 2×10^{-4} s.

The main difference between the excitation circuits consists in the methods used to isolate the power supply circuits of the SSD and NSSD.

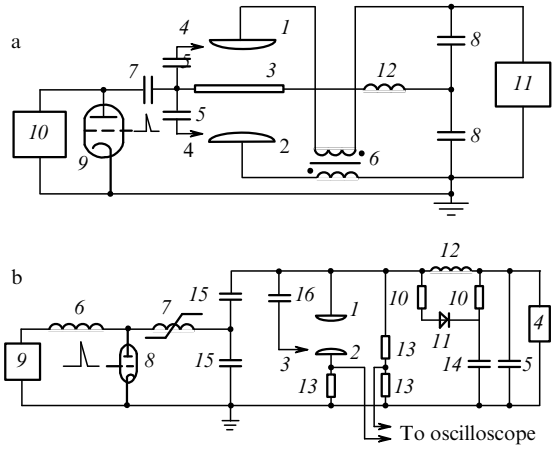

Figure 1. Schematic diagrams of the circuits for exciting a combined discharge (a) with and (b) without an auxiliary electrode. (a): (*1*, *2*) electrodes; (*3*) auxiliary electrode; (*4*) ignitor electrodes; (*5*) discharge capacitors; (*6*) pulse transformer; (*7*) capacitor; (*8*) storage capacitors of the power supply; (*9*) TGI-1000/25 thyratron; (*10*) laser power supply; (*11*) power supply of the ignition circuit; (*12*) inductance. (b): (*1*, *2*) electrodes; (*3*) ignitor electrode; (*4*) laser power supply; (*5*) storage capacitor; (*6*) inductance; (*7*) variable inductance; (*8*) TGI-1000/25 thyratron; (*9*) power supply of the ignition circuit; (*10*) resistors; (*11*) diodes; (*12*) inductance; (*13*) resistors for measuring the discharge current; (*14*) additional storage capacitor; (*15*) discharge capacitors; (*16*) ignition capacitors.

In the first circuit (Fig. 1a), these supply circuits are isolated by placing an auxiliary electrode (*3*) in the interelectrode gap. In this case, plasma is produced in the gap (*1*–*2*) by a simultaneous ignition of two parallel discharges in gaps (*1*–*3*) and (*3*–*2*). The currents in these gaps are equalized using a pulse transformer (*6*).The current flow through the gap (*1*–*3*–*2*) at the NSSD stage is ensured by a capacitive storage (*8*).

When using this circuit, the dimensions of the active medium were $4.5 \times 2.8 \times 80$ cm (with interelectrode gap widths of 2.25 cm). A TGI-1000/25 thyratron served as a switch (*9*). The ignitor electrodes (*4*) were manufactured of a foiled glass-cloth laminate 1.5 mm thick; and the width of the sections spaced by 0.5 mm was 1.5 mm. The total capacitance of capacitors (*5*) was 1.4 nF, the capacitances of capacitor (*7*) and of capacitors (*8*) were 2 nF and 20 μF, respectively. A pulse transformer (*6*) consisted of 20 turns of a coaxial cable wound on a ferrite ring measuring $\varnothing 10/\varnothing 6 \times 1.5$ cm. The inner conductor and the braid of the coaxial cable were used as the primary and secondary windings, respectively.

The second circuit (Fig. 1b) uses a diode–inductive isolation of the feed circuits. The presence of diodes (*11*) in the feed circuit of the NSSD is necessary for maintaining the discharge current at the most crucial moment of the discharge development, when the SSD current terminates and the NSSD current rise is limited by an inductance (*12*). Setting such a diode chain makes it possible to increase the maximum energy supplied to the gas at the NSSD stage by more than 50 %.

The characteristics of a CO_2 laser with the latter excitation circuit were studied for an active medium with dimensions of $4 \times 3.1 \times 80$ cm. The total capacitance of capacitors (*16*) was 1 nF. The capacitances of the main (*5*) and additional (*14*) storages were 8 and 0.5 μF, respectively. The diode assembly consisted of twenty-two KTs201E diodes connected in parallel, and the inductance (*12*) was 10 μH.

Analysis of the excitation circuits shows that the first circuit (Fig. 1a) is the most promising, because, due to the low inductance of the current transformer with the windings connected in the counter directions, this circuit has no special current-limiting elements. However, because we failed to make the auxiliary electrode transparent, each gap has its individual cathode potential drop. Probably, for this reason, the discharge energy characteristics obtained using the second excitation circuit were found to be 10 % higher than those for the first circuit. Thus, in the subsequent analysis, we present the results of investigations performed using the second circuit. Nevertheless, we believe that the former will be more promising for exciting the active medium in wider interelectrode gaps, where the fraction of energy dissipated in the cathode layer decreases.

3. Model for calculating the laser characteristics

To calculate the laser characteristics, we should construct a model that can take into account the vibrational excitation kinetics, the exchange and relaxation of the vibrational energy, and the generation of electromagnetic waves as applied to the conditions for exciting the active medium by a combined discharge.

This model is based on a system of balance equations for electrons, ions (O^-, CO_3, CO_2^+, N_2^+, and He^+), and neutral components of the gas medium: N_2 ($v = 1 - 5$), CO_2 (00^01), CO_2 (01^00), CO_2 (02^00), CO_2 (03^00), CO_2 (10^00). We used plasmochemical and vibrational relaxation reactions presented in papers [12, 13]. The rate constants of the reactions involving electrons, which depend on the field strength, were calculated using the Boltzmann equation. The form of this equation and the numerical scheme for its solution are presented in Ref. [13]. The balance equations for photons were also included in the system to describe the generation process.

The system was solved numerically by the third-order-precision Rosenbrock method [14]. The calculations were carried out successively in two steps. At the first step, the ionisation occurring at the SSD stage was calculated. At the second step, when the electron concentration n_e reached a value n_e^{max}, the field strength E corresponding to the NSSD stage was specified. The concentration n_e^{max} was determined from the condition

$$e\mu_e E^2 \int_0^\infty n_e(t)\mathrm{d}t = w_0\,, \qquad (1)$$

where w_0 is the preset specific energy input, μ_e is the electron mobility, and $n_e(0) = n_e^{max}$.

This step also involved the calculation of the basic parameters of laser generation and kinetic processes in the active medium of a CO_2 laser.

4. Time characteristics

Oscillograms of SSD current pulses ionising the active medium and NSSD current pulses ensuring the input of the greater part of energy into the gas at the plasma decay stage and oscillograms of the voltages at the electrodes during the NSSD are shown in Fig. 2. These oscillograms correspond to a packet of four successive pulses with a separation of 100 μs (the packet repetition rate is 1250 Hz, the gas mixture composition is $CO_2 : N_2 : He = 1 : 6 : 15$, and the mixture pressure is 60 Torr). The analysis of the ratio of the energies transferred to the gas mixture at the SSD and NSSD stages shows that, in typical regimes, this ratio is 0.01 – 0.03.

These oscillograms show that the amplitude of NSSD current pulses in a packet initially rises and then falls. In our opinion, this fall is determined by the production of electronegative components (such as O_2, NO_2, N_2O, and NO) in the medium, which increase the attachment rate and reduce the discharge current [15].

It is interesting that, if the number of pulses in a packet does not exceed three, the total duration of radiation pulses changes insignificantly. This fact is confirmed by the oscillograms of radiation pulses shown in Fig. 3. The input energy was 130, 170, and 200 J L^{-1} atm^{-1} at a pulse-packet repetition rate of 400 Hz. A gas mixture with a composition $CO_2 : CO : N_2 : He = 1.5 : 1.8 : 8.5 : 19$ at a pressure of 60 Torr was used. The oscillogram of the radition pulses corresponding to three pulses in the packet was obtained at a lower initial voltage caused by an impaired discharge stability. It should be noted that, as the number of pulses in a packet increases and the energy supplied to the gas rises by a factor of 2 – 3, the radiation energy increases by a factor of only 1.4 – 1.5. This effect is evidently associated with the gas heating.

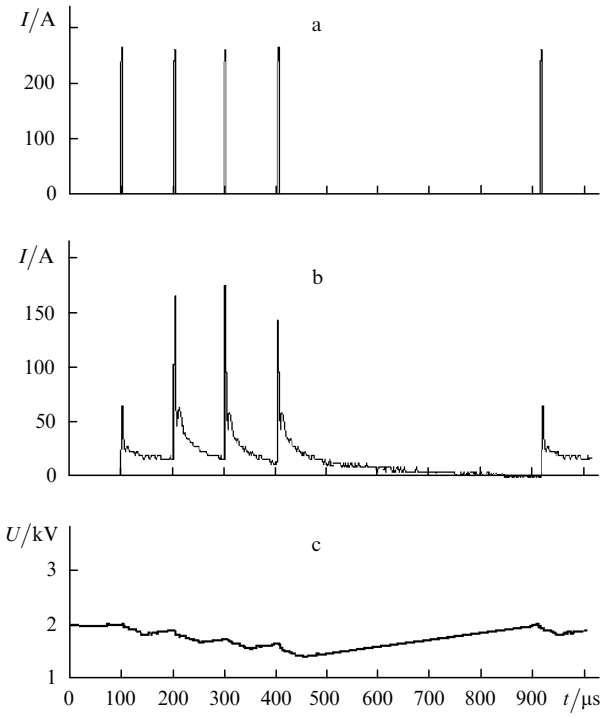

Figure 2. Oscillograms of the current I between the electrodes for (a) a SSD, (b) an NSSD, and (c) the voltage U of the NSSD.

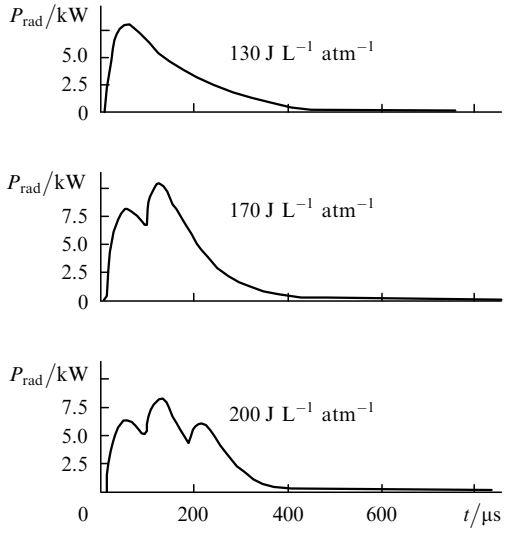

Figure 3. Typical oscillograms of radiation pulses corresponding to one, two, and three pump pulses in a packet.

It should be emphasized that the peak radiation power reaches ~ 10 kW at a mean power of ~ 1 kW, and the pulse shape can be varied. These circumstances are very important for industrial applications of the laser.

5. Energy characteristics

When comparing the lasers excited by different methods, the primarily compared parameters are the lasing efficiency and specific energy characteristics. We analysed numerically the most popular laser excitation methods: a continuous SSD, a continuous NSSD with an optimal field strength for

the energy transfer to the upper laser level, and a pulsed NSSD with an exponentially decaying current (at a constant and optimal field). The ratio E/N (N is the concentration of gas particles) for a SSD was chosen from the condition

$$K_0 N_{CO_2} + \beta N_{ion} = K_{CO_2} N_{CO_2} + K_{N_2} N_{N_2} + K_{He} N_{He}, \quad (2)$$

where K_0 is the dissociative attachment constant; β is the recombination coefficient; K_j and N_j are the ionisation constants, which are functions of E/N and concentration of the jth gas component; $j = CO_2$, N_2, He; and N_{ion} is the total ion concentration.

The results of calculations are presented in Fig. 4 as dependences of the lasing efficiency on the specific energy transferred to the medium in the course of gas circulation through the laser active zone. One can see that the highest efficiency is achieved in the pulse mode [curve (*1*)]. The differences in the laser operation efficiency upon pumping by pulsed and continuous NSSDs [curves (*2*) and (*3*)] are determined mainly by the loss due to the V–T relaxation. The laser efficiency additionally decreases, when the active medium is pumped by a SSD [curve (*4*)] due to the fact that the value of E/N is not optimal for the energy transfer to the upper laser level. Note, however, that the latter difference decreases with increasing electrode spacing [16].

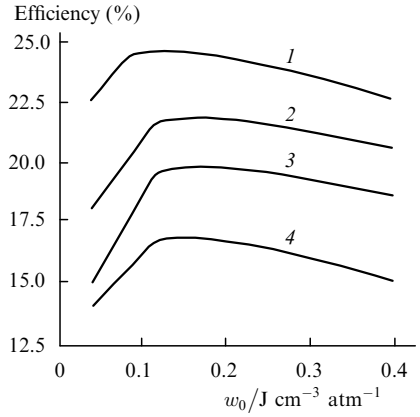

Figure 4. The CO_2-laser efficiency as a function of specific input energy w_0 pumped by (*1*) a combined discharge in a pulse mode, an NSSD with a width of electrodes of (*2*) 3.5 and (*3*) 5 cm, and (*4*) a continuous SSD. A $CO_2 : N_2 : He = 1 : 4 : 8$ mixture composition, a pressure of 0.1 atm, and a circulation velocity of 50 m s^{-1} are used.

Thus, for the same mean power dissipated in the gas, the pumping of a repetitively pulsed CO_2 laser by a combined discharge ensures a higher efficiency and better energy characteristics than other methods considered above.

Fig. 5 shows the experimental dependence of the laser efficiency on the number of laser pulses measured for an optimal energy input of 0.15 J cm^{-3} atm^{-1}. The maximum efficiency is 22 %, which agrees well with the results of calculations performed neglecting the energy loss in the region of the cathode potential drop. A rapid fall of the efficiency from 22 % to 12 % with increasing the number of laser pulses from 10^4 to 3×10^5 deserves attention. The reasons for such a fall are not quite clear and are probably associated with a decrease in the CO_2 concentration and with the formation of its dissociation products: CO, O_2, and

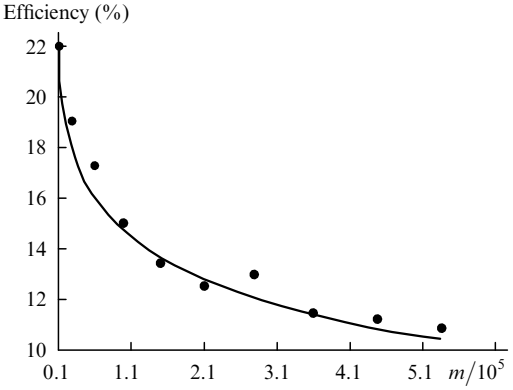

Figure 5. The efficiency of a CO_2-laser excited by a combined discharge and operating in the sealed-off regime as a function of the number of pulses m for a $CO_2 : N_2 : He = 1 : 4 : 8$ mixture composition at a pressure of 80 Torr.

nitrogen oxides that reduce the mean output power and lasing efficiency [15]. Therefore, in subsequent experiments, the input and output energies were measured after 10^6 laser pulses (unless otherwise indicated).

Fig. 6 shows the results of experiments aimed at the selection of the gas mixture composition. These measurements were performed at a pulse repetition rate of 700 Hz for initial laser pulses [curves (*1–4*)] and after 10^6 pulses [curve (*2*)]. Note that, as the CO_2 content in the gas mixture increased, the power dissipated in the gas decreased [curve (*4*)]. For initial pulses, the maximum radiation power [curve (*3*)] was obtained for a mixture with a composition $CO_2 : N_2 = 1 : 4$. However, after 10^6 pulses, the mixtures with a ratio of concentrations $[CO_2]/([CO_2] + [N_2]) < 0.1$ were found to be optimal. Probably, this effect is explained by the reasons similar to those determining a decrease in the efficiency at the initial stage of laser operation. As the He content in the gas mixture rises, the input and output powers and the laser efficiency increase and then reach saturation [curve (*5*)].

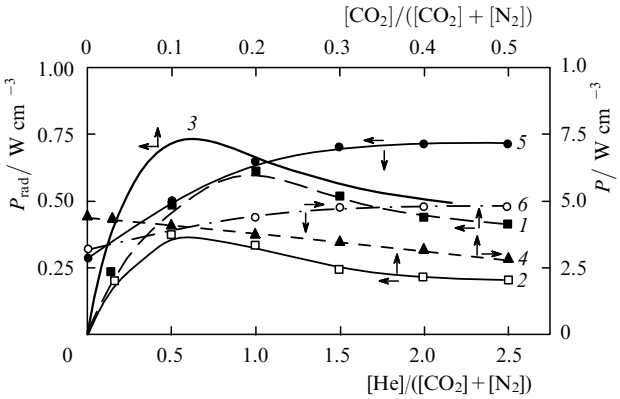

Figure 6. Experimental (*1*, *2*, *4–6*) and calculated (*3*) dependences of the (*1–3*, *5*) specific mean radiation power P_{rad} and (*4*, *6*) specific mean power of an NSSD (pump power) P on the concentration ratios (*1–4*) $[CO_2]/([CO_2] + [N_2])$ and (*5*, *6*) $[He]/([CO_2] + [N_2])$ obtained (*1*, *3–6*) during the initial pulses and (*2*) after 10^6 pulses at (*1–4*) a partial helium pressure $p_{H_2} = 40$ Torr, a pressure of the $CO_2 - N_2$ mixture $p = 30$ Torr, and a pulse repetition rate $f = 700$ Hz and at (*5*, *6*) a pressure $p = 20$ Torr of the $CO_2 : N_2 = 1 : 4$ mixture composition and $f = 800$ Hz.

Within a gas pressure range of 40–80 Torr, the saturation occurs at a ratio $[He]/([CO_2]+[N_2]) = 1.5-2$ almost regardless of the $[CO_2]/[N_2]$ ratio. This value slightly differs from that obtained for lasers operating at atmospheric pressure [17], for which the optimal value of the $[He]/([CO_2]+[N_2])$ ratio is ~ 0.67. The high helium concentration in the lasers under study with gains that are lower than those of TEA lasers can be explained by a more significant role of the kinetics of relaxation processes. In particular, an accelerated depopulation of the lower laser level is required in our case in order to maintain the gain at a level above its threshold value during the plasma decay for as long time as possible. As is known, this is achieved by raising the rate of depopulation of the lower laser level through an increase in the helium concentration.

The values of the pump and radiation power averaged over the period are important characteristics for the practical application of a repetitively pulsed laser. These parameters as functions of the pulse repetition rate at various gas-mixture compositions are shown in Fig. 7.

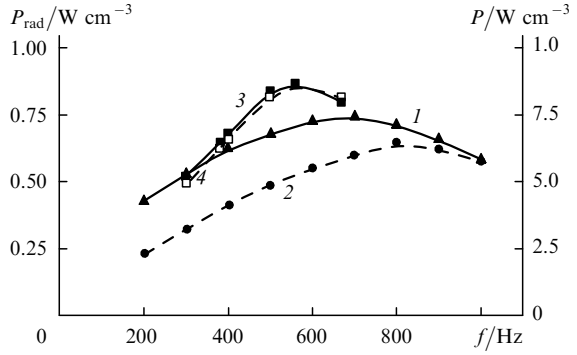

Figure 7. Powers (*1*, *3*) P_{rad} and (*2*, *4*) P versus pulse repetition rate f for (*1*, *2*) the $CO_2 : N_2 : He = 1 : 4 : 8$ mixture composition at $p =$ 70 Torr for the initial pulses and (*3*, *4*) the $CO_2 : CO : N_2 : He =$ $1 : 0.7 : 10 : 20$ composition at $p = 60$ Torr after 10^6 pulses.

Because the pump power increases linearly with the pulse repetition rate in a range of low repetition rates (400–500 Hz), the output power also rises linearly in this range. At higher frequencies, these functions become saturated, which is accompanied by decrease in the power supplied to the gas and, consequently, in the output power. In our experiments, a stable maximum of the energy input to the NSSD was observed at frequencies of 600–800 Hz for $CO_2 - N_2 - He$ mixtures and 400–600 Hz for CO-containing mixtures.

A decrease in the pump power which leads to the reduction of the output power, is probably explained by the effect of gas-dynamic plugs and near-electrode processes on the discharge stability [18]. A certain decrease in the laser efficiency with increasing pulse repetition rate is evidently caused by a deterioration of the discharge plasma homogeneity and the appearance of the laser gain nonuniformity along the cavity axis, which leads to a decrease in the radiation extraction efficiency at a constant cavity Q factor.

Fig. 8 shows dependences of the mean pump and output powers on the mixture pressure. The decrease in the output power after its maximum (at a constant pump power), can be caused by a decrease in the gain due to the collisional broadening of the $00^01 \sim 10^00$ spectral line in CO_2 molecules. This process prevails at pressures above 60 Torr.

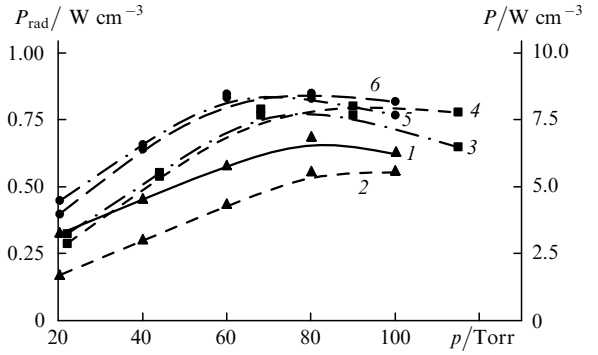

Figure 8. Powers (*1*, *3*, *5*) P_{rad} and (*2*, *4*, *6*)P versus pressure p of the working gas mixture for the initial pulses with the (*1*, *2*) $CO_2 : N_2 : He$ $= 1 : 3 : 6$, (*3*, *4*) $CO_2 : N_2 : He : H_2 = 1 : 3 : 6 : 1$, and (*5*, *6*) $CO_2 : CO$ $: N_2 : He = 1 : 0.7 : 10 : 20$ mixture compositions at $f = 500$ Hz.

Fig. 9 presents the dependences of the ultimate specific energy w supplied to the gas in an NSSD pulse on the repetition rate of SSD pulses (a single pulse in a packet) for various compositions and pressures of the gas mixture. The curves can be conventionally divided into two parts: a linear segment up to a frequency of 500–700 Hz and a portion where w abruptly falls at higher frequencies. A plateau existing at comparatively low energy inputs [curves (*3*–*5*)] qualitatively agrees with the known theory of a repetitively pulsed discharge [18, 19] based on the influence of gas-dynamic plugs and heated near-electrode layers on the discharge stability. It is assumed that, as a consequence of the current passage through the discharge gap, the gas is heated and expands (equalises its pressure) in both directions along the gas flow. A corresponding interval between the pulses is necessary for all the discharge-produced gas-density inhomogeneities to be removed by the gas flow.

This is confirmed well by curves (*4*–*6*) obtained at various gas-flow velocities and all other factors being the same. One can see that the constant energy inputs begin drastically decrease, when the gas propagates a distance

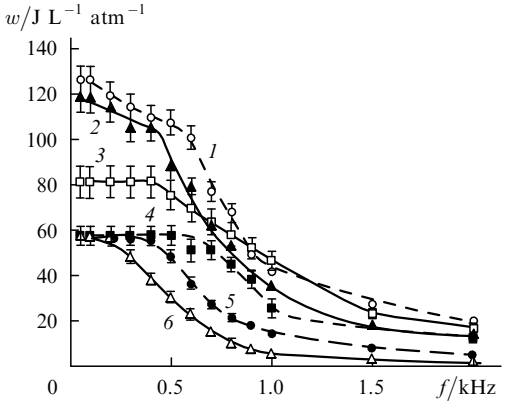

Figure 9. The ultimate specific energy w supplied to the gas during an NSSD pulse as a function of the pulse repetition rate f (a single pulse in a packet) for gas flow velocities through the discharge gap of (*1*–*4*) 50, (*5*) 40, and (*6*) 25 m s^{-1} and for various gas mixture compositions and pressures: (*1*) $CO_2 : CO : N_2 : He = 1.5 : 1 : 10 : 22$, $p = 70$ Torr; (*2*) $CO_2 : N_2 : He : H_2 = 1 : 4 : 8 : 1$, $p = 88$ Torr; (*3*) $CO_2 : N_2 : He : H_2$ $= 1 : 3 : 6 : 1$, $p = 66$ Torr; and (*4*–*6*) $CO_2 : N_2 : He = 1 : 3 : 6$, $p =$ 60 Torr.

shorter than 10 cm during the time interval between pulses, which corresponds a threefold replacement of the gas in the discharge gap. At higher energy inputs [curves (*1*) and (*2*)], no plateau is observed. This fact is evidently a manifestation of an additional discharge contraction mechanism and is analysed below.

6. Effect of H_2 and CO impurities on the laser characteristics

Impurities of CO and H_2 molecules added to $CO_2 - N_2 -$ He gas mixtures are widely used in CO_2 lasers. As is known [17], such impurities appreciably increase the service-life characteristics of sealed-off CO_2 lasers. Therefore, let us consider the effect of impurities mainly on the laser energy characteristics.

The results presented in Fig. 9 [curves (*1–3*)] show that H_2 and CO admixtures added to a $CO_2 - N_2 -$ He mixture increase the ultimate energy input by $\sim 50\,\%$ at all pulse repetition rates.

At the same time, the mechanisms of increasing the energy characteristics of discharges with CO and H_2 admixtures are apparently different. The influence of CO added to a CO_2-based gas mixture was discussed earlier in [15] and was attributed to a decrease in the concentration of electronegative components that are produced in the discharge through the reactions

$$CO^* + O \rightarrow CO_2, \quad NO + CO \rightarrow N_2 + CO_2\,, \tag{3}$$

$$O^* + CO \rightarrow CO_2, \quad N_2O + CO \rightarrow N_2 + CO_2\,, \tag{4}$$

$$NO_2 + CO \rightarrow N_2 + CO_2\,. \tag{5}$$

An increase in the ultimate energy inputs was earlier observed in Ref. [20] upon additions of triethylamine and NH_3 to N_2, $CO_2 - N_2$, and CO_2. This effect was explained by a reduction of the rates of stepwise ionisation through the $A^3\Sigma_u^+$ and $B^3\Pi_g$ states of nitrogen molecules. Probably, similar processes may also occur in our case upon adding H_2. To substantiate this assumption, consider in more detail the effect of addition of H_2 molecules on the energy characteristics of a CO_2 laser. The interaction cross sections of H_2 molecules are known rather well.

The dependence of the ultimate energy w dissipated in the gas mixture at the NSSD stage on the partial hydrogen pressure p_{H_2} is shown in Fig. 10. As p_{H_2} is increased up to 20 Torr, the ultimate energy w sharply increases independently of the mixture composition. A further increase in p_{H_2} causes no noticeable increase in w. The explanation of the causes responsible for the rise w seems to be very important. As was mentioned earlier, this can be determined by the fact that, as the H_2 concentration increases, the direct and stepwise ionisation rates decrease, leading to a discharge contraction.

This assumption was verified by calculating the excitation and ionisation constants for the excited states of nitrogen molecules using the Boltzmann equation. Based on the equality of the constants mentioned above, we calculated the ultimate E/p values of the positive column of an NSSD as a function of the partial hydrogen pressure (Fig. 10, solid curve) for a mixture with a $CO_2 : N_2 : He = 1 : 4 : 7$ composition at a pressure of 50 Torr. A good agreement between the calculated and experimental data

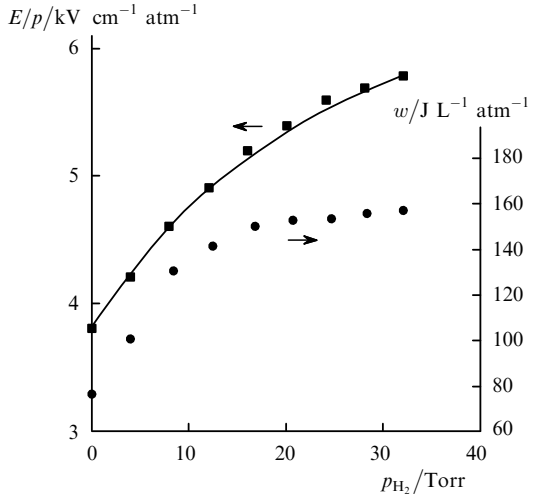

Figure 10. Calculated (curve) and experimental (dots) ultimate ratios E/p (■, solid curve) and ultimate specific energy w (●) of an NSSD versus partial H_2 pressure for a $CO_2 : N_2 : He = 1 : 4 : 7$ mixture composition at $p = 50$ Torr.

indicates that, reducing the stepwise ionisation rate, hydrogen suppresses the development of instabilities.

Fig. 11 shows the influence of H_2 and CO impurities on the input and output energy. One can see that the radiation energy peak corresponds to a partial hydrogen pressure of $p_{H_2} \sim 3 - 5$ Torr. A further increase in p_{H_2} leads to a fall of the output energy, although the input energy continues rising [Fig. 11, curves (*4–6*)] up to $p_{H_2} = 30$ Torr. This occurs due to the fact that, after the peak is passed over, the energy supplied to the gas does not compensate for the increasing depopulation rate of the upper laser level caused by the rising concentration of H_2.

As the partial pressure of CO rises, the output energy maximum is observed at somewhat lower pressures than the maximum of the input energy. With a further increase in the CO pressure, a slight fall of the input energy and a signifi-

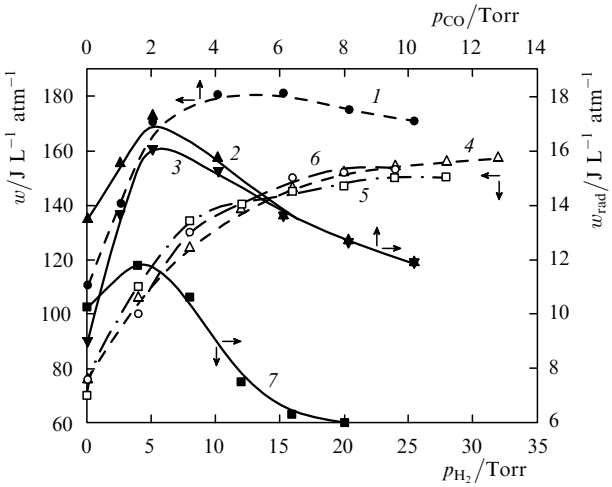

Figure 11. Specific input (w; *1*, *4–6*) and output (w_{rad}; *2*, *3*, *7*) energies per pulse versus partial pressures p_{CO} (*1–3*) and p_{H_2} (*4–7*) measured (*1*, *2*, *4–7*) for the initial pulses and (*3*) after 10^6 pulses at $f = 500$ (*1–3*) and 200 Hz (*4–7*) for various gas mixture compositions and pressures: (*1–3*) $CO_2 : N_2 : He = 1 : 4 : 8$, $p = 60$ Torr; (*4*) $CO_2 : N_2 : He = 1 : 4 : 5$, $p = 80$ Torr; (*5*) $CO_2 : N_2 : He = 1 : 3 : 6$, $p = 60$ Torr; and (*6*, *7*) $CO_2 : N_2 : He = 1 : 4 : 7$, $p = 50$ Torr.

cant fall of the output energy are observed. The latter is caused by a decrease in the laser gain, because CO_2 and CO molecules are rivals from the viewpoint of energy absorption. In the case of a constant cavity Q factor, this causes a decrease in the generated radiation power.

These experiments allowed us to determine that, in the mixture with a $CO_2 : CO : N_2 : He = 1.5 : 1 : 8.5 : 19$ composition at a pressure of 60 Torr and a power of 10 W cm^{-3} supplied to the gas, a decrease in the radiated power was within 10 % of the maximum during the operational period (3×10^7 pulses) in the sealed-off regime.

7. Conclusions

An industrial combined-discharge-pumped CO_2 laser of a new generation has been built. The laser is capable of operating in the repetitively pulsed regime with the pulse shape and duration being varied. In the industrial sealed-off laser, a mean radiation power of 1 kW and a peak power of 10 kW per litre of the active medium are obtained.

The specific mean radiation power and the peak power amounts to 10 and 100 W cm^{-3}, respectively.

The laser has high operational efficiencies: 22 % in the regime of complete gas replacement (for the initial pulses), 28 % by neglecting the energy loss in the region of cathode potential drop, and ~ 10 % in the sealed operational regime with CO-containing mixtures.

Small additions of H_2 lead to an increase in the input and output energies by 50 %. The mixture compositions, gas pressures, and repetition rates of laser pulses optimal for reaching the maximum radiation energy are determined.

Note that the high reliability of the laser operation was tested in experiments on the production of nanometer-size fine Y_2O_3-stabilized Al_2O_3 and ZnO_2 powders. However, the reasons for a rapid decrease in the laser efficiency from 22 to 12 % after $\sim 3 \times 10^5$ pulses in the sealed regime remain unclear.

References

1. Bychkov Yu.I., Korolev Yu.D., Mesyats G.A., et al. *Inzhectsionnaya gazovaya elektronika* (Injection Gas Electronics) (Novosibirsk: Nauka, 1982).
2. Napartovich A.P., Naumov V.G., Shaisov V.M. *Pis'ma Zh. Tekh. Fiz.*, **3**, 349 (1977).
3. Bychkov Y.I., Osipov V.V., Telnov V.A. *J. Physique*, **40**, 161 (1979).
4. Reilly J.R. *J. Appl. Phys.*, **41**, 3411 (1972).
5. Hill A.B. *Appl. Phys. Lett.*, **22**, 670 (1973).
6. Generalov N.A., Zimakov V.P., Kosynkin V.D., Roitenburg D.I. *Fiz. Plasmy*, **3**, 626 (1977).
7. Osipov V.V., Savin V.V., Tel'nov V.A. *Zh. Prikl. Mekh. Tekh. Fiz.* (2), 10 (1982).
8. Nikumb S.K., Seguin H.J.J., Seguin V.A., Wills R.J., Reshef H.W. *IEEE J. Quantum Electron.*, **25**, 1725 (1989).
9. Osipov V.V., Ivanov M.G., Mekhryakov V.N., RF Patent No. 2107366, 20 March 1998; *Byull. Izobr.*, (8), 498 (1998).
10. Osipov V.V., Ivanov M.G. RF Patent No. 212455, 27 December 1998; *Byull. Izobr.*, (36), 423 (1998).
11. Korenev V.N., Kushch N.P., Skivko G.P., Osipov V.V., Tel'nov V.A. USSR Inventor's Certificate No. 1238670, 27 July 1984.
12. Taylor R.L., Bitterman S. *Rev. Mod. Phys.*, **41**, 26 (1969).
13. Smith K., Tomson R. *Computer Modeling of Gas Lasers* (New York: Plenum, 1978; Moscow: Mir, 1981).
14. Rakitskii Yu.V., et al. *Chislennye metody resheniya zhestkikh sistem* (Numerical Methods for Solving Rigid Systems) (Moscow: Nauka, 1979).
15. Karpov V.M., Konev Yu.G., Orlovskii V.M., Osipov V.V., Ponomarev V.B. *Kvantovaya Elektron.*, **15**, 465 (1988) [*Sov. J. Quantum Electron.*, **18**, 294 (1988).
16. Judd O.P., Wada J.Y. *IEEE J. Quantum Electron.*, **10**, 12 (1974).
17. Mesyats G.A., Osipov V.V., TarasenkoV.F. *Impul'snye gazovye lazery* (Pulsed Gas Lasers) (Moscow: Nauka, 1991).
18. Dzacowic G.S., Wutzke S.A. *J. Appl. Phys.*, **46**, 5061 (1973).
19. Velikhov E.P., Baranov V.Yu., Letokhov, V.S., Ryabov E.A., Starostin A.N. *Impul'snye CO_2-lazery i ikh primenenie dlya razdeleniya izotopov* (Pulsed CO_2 Lasers and Their Application to Isotope Separation) (Moscow: Nauka, 1983).
20. Prokhorov A.M., Semenov S.K., Firsov K.N. *Kvantovaya Elektron.*, **15**, 553 (1988) [*Sov. J. Quantum Electron.*, **18**, 351 (1988).